Cohesive, electronic, and structural properties of Al_3Li: An important metastable phase

X.-Q. Guo, R. Podloucky,* Jian-hua Xu, and A. J. Freeman
Department of Physics and Astronomy, Northwestern University, Evanston, Illinois 60208-3112
(Received 28 December 1989)

The cohesive and electronic properties and the structural stability of Al_3Li in its fcc-based $L1_2$ and bcc-based $D0_3$ structures are investigated with use of the first-principles all-electron full-potential linear augmented-plane-wave (FLAPW) method. Particular care was taken to ensure convergence of the total energy as a function of the inherent numerical parameters in order to obtain high precision. To further understand the calculated stability, the electronic structure of some superstructures (notably Al_7Li and Al_5Li_3) was also determined. The equilibrium properties of the metastable $L1_2$ structure are in good agreement with experiment. A simple picture emerged which emphasizes the importance of the anisotropic bonding between the Al atoms with the Li basically donating its valence electron to strengthen the Al bonds. The bulk moduli were found to decrease with increasing Li content; by contrast, the calculated Young's modulus of the $L1_2$ phase is high (1.20 Mbar) compared to the bulk modulus (0.72 Mbar). Both results are in keeping with the picture of anisotropic Al—Al bonding.

I. INTRODUCTION

In the search for new light-weight materials for aerospace applications, Al-Li alloys have attracted strong attention in the past decade due to a combination of low density and high stiffness. No other aluminum alloys can compete in that respect.[1,2] One of the interesting aspects of Al-Li alloys is the occurrence of the metastable δ' Al_3Li phase, which forms as precipitates having the $L1_2$ (Cu_3Au) structure. The δ' phase is coherent with the fcc Al-Li matrix (i.e., α phase) and may occupy up to 50% of the volume when a high-cooling-rate technique is applied.[3] The technological problem is to produce high-stiffness materials with suitable mechanical properties; for the Al-Li alloys, the δ' phase plays an important role, as has been widely studied by numerous experimental techniques.[4] The intrinsic properties of the δ' phase certainly play an important role in determining the mechanical properties of the alloy. Since the structural and mechanical properties of an intermetallic compound are closely linked to its electronic structure, we performed a detailed study on the electronic structure of crystalline Al_3Li. Furthermore, because of the metastability of the δ' phase and its formation via precipitation, it is difficult or even impossible to obtain accurate experimental determinations of its intrinsic properties. Therefore, a reliable first-principles study is a useful tool to support the experimental efforts. Last but not least, because of the subtle phase stabilities of Al-Li alloys as indicated by the metastability of Al_3Li, a precise method is needed in order to obtain reliable results about the energetics and equilibrium properties.

In order to elucidate the structural competition, we study the electronic structure and energetics of the fcc-type δ' phase and another, artificial bcc-type structure by application of a precise first-principles electronic-structure method. Some results of a previous supercell study[5] are also used in the discussion. The present paper is a part of an extensive study of the Al-Li system which also tries to calculate a complete phase diagram[6] from first principles. The ordered LiAl compounds were already investigated by us[7] and we further exploit these results in the present paper.

In Sec. III the results of the total-energy calculation as well as a detailed analysis of the electronic structure are presented. In Sec. IV we discuss the results for Al_3Li in connection with the phase diagram of Al-Li. As an Appendix, we compare our calculated full-potential linear augmented-plane-wave (FLAPW) results and some separately calculated linear muffin-tin orbital (LMTO) results with those published previously[8] using an augmented-spherical-wave (ASW) approach for the δ' phase.

II. COMPUTATIONAL DETAILS

The self-consistent FLAPW method[9] was applied to calculate the electronic structure and volume-dependent total energies of Al_3Li compounds as well as related fcc superstructures (Al_7Li, Al_6Li_2, Al_5Li_3) as applied in an earlier study.[5] For Al_3Li, two different structures were investigated, the fcc-type $L1_2$ and the bcc-type $D0_3$ (cf. Fig. 1). The muffin-tin spheres were chosen to be 2.58 a.u. for both atomic species. The spherical harmonic expansion of charge density and potential inside the muffin-tin spheres was done up to $l=8$. For the interstitial region, an expansion of about 2000 plane waves were used. More than 200 LAPW basis functions (50 per atom) were used in the band calculation, which turned out to be sufficient to get accurate results for the total energies and their derivatives because of the rather plane-wave-like nature of the wave functions—as also found for LiAl.[7] From all these expansions, we estimate the er-

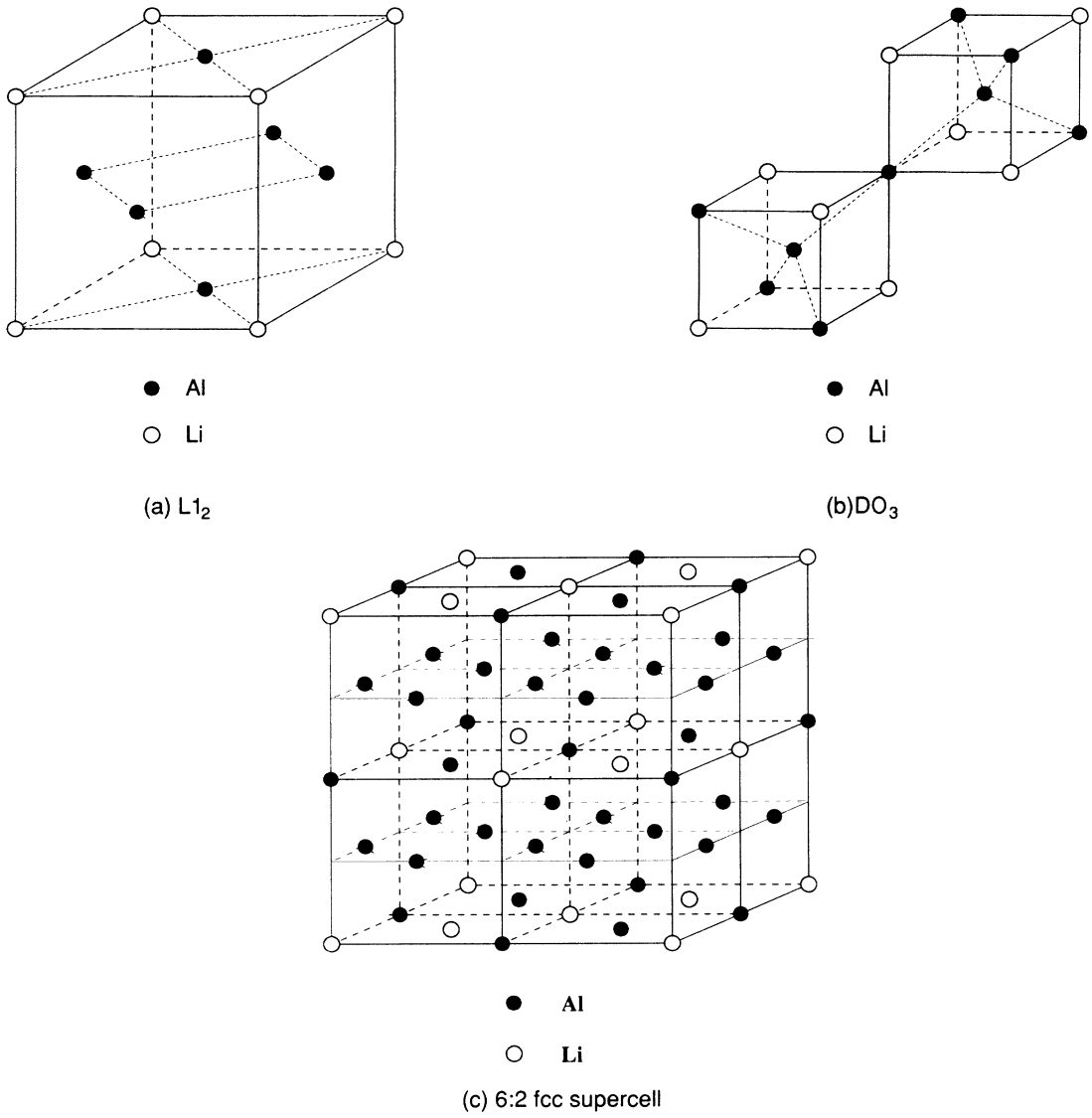

FIG. 1. Cubic unit cells of (a) the $L1_2$ crystal structure, (b) DO_3 crystal structure, and (c) fcc supercell.

ror in the total energy to be smaller than 0.15 mRy. Because of some surprising results obtained in a recent study employing the ASW method,[8] we tested our FLAPW results by increasing the basis size by a factor of 2. As a result of this test, the total energy was lowered by 0.1 mRy, and its first and second derivatives (yielding equilibrium spacing and bulk modulus) remained unchanged.

Since there are no uncontrolled numerical parameters in the FLAPW method, special care was taken to investigate all other inherent numerical parameters such as the dependency of the total energy on the number of **k** points, $E(n_{\mathbf{k}})$, used in the linear tetrahedron method for the Brillouin-zone integration. The number of **k** points, $n_{\mathbf{k}}$, is crucial for the precision of the absolute total energy, especially for comparing total energies of different structures. By systematically increasing the number of **k** points from 30 to 250 and extrapolating the results to infinity, we obtained convergence to better than 0.1 mRy for $E(n_{\mathbf{k}})$. In a similar way we could obtain a comparable precision for the supercell results.[5] Finally, to crosscheck our FLAPW results for the $L1_2$ structure of Al_3Li, the LMTO method[10] was applied, as discussed in more detail in the Appendix. In all calculations the Hedin-Lundqvist ansatz[11] for the local-density approximation to the exchange-correlation potential was taken.

III. RESULTS

A. Total energies and equilibrium properties

Figure 2 compares the calculated total energies as a function of volume (or Wigner-Seitz radius as shown in the graph) of Al_3Li (denoted henceforth as a 3:1 compound). The lowest curve corresponds to the stable fcc-type $L1_2$ structure [Fig. 1(a)], whereas the highest one be-

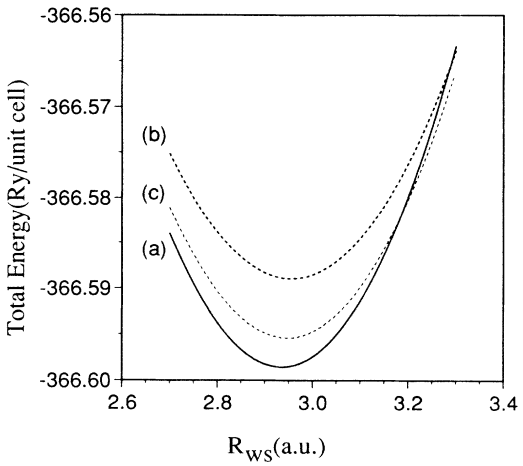

FIG. 2. Total energy per atom for Al_3Li vs atomic radius in (a) the $L1_2$ (solid line) and (b) $D0_3$ (thick-dashed line) structures, and (c) for a fcc supercell of Al_6Li_2 composition (thin-dashed line).

longs to the bcc-type $D0_3$ structure [Fig. 1(b)]. Table I illustrates the instability of the $D0_3$ case because it shows a positive formation energy. This table also shows that $L1_2$ is more stable than $D0_3$ by 10 mRy/atom. For $D0_3$ the bulk modulus is also substantially lower (even lower than that of the corresponding $B32$ structure of LiAl), and the atomic (or Wigner-Seitz) radius is expanded, thereby reflecting the decrease of bonding as compared to $L1_2$. For the 1:1 Al-Li compounds[7] the situation is reversed because then the bcc-type $B32$ structure (which one obtains by replacing the center Al atom of $D0_3$ by Li in Fig. 1(b) is lower in total energy per atom by 6.8 mRy when compared to the corresponding fcc-type $L1_0$ structure [as constructed by replacing the center Al atoms of two parallel faces in Fig. 1(a) by Li]. As shown in more detail in the next subsection, this change of structural stability as a function of composition is due to the change in anisotropy of Al bonds based on the model assumption that Li basically transfers its valence electron in between the Al atoms and strengthens the Al-Al bonds.[7] For Al_3Li, a fcc-bcc structural transition is not possible because the total-energy curves do not cross at any realistic pressure. The situation is somewhat different for the LiAl cases. Although a direct $B32$-$L1_0$ transition cannot be forced, an indirect transition via a mediator $B2$ phase could be possible because its total energy crosses both the $B32$ and $L1_0$ curves.

Figure 2 also presents a total-energy versus volume curve for a second 3:1 (or rather 6:2) fcc compound ("Al_6Li_2"). This structure can only be realized by employing an eight-atom supercell [cf. Fig. 1(c)]. Essentially it is similar to the $L1_2$ geometry, but with a shift by a nearest-neighbor distance perpendicular to the Al-atom chain located in one of the mixed Al-Li faces [e.g., top face in Fig. 1(a)]. Although the structural difference seems to be small, the energetics are quite different. As compared to $L1_2$, this artificial superstructure is less stable, by 3.3 mRy per atom, and it has a slightly larger equilibrium lattice parameter (0.5%) but a substantially reduced bulk modulus (15%). Because the eight-atom supercell has a much higher statistical weight (it represents 24 configurations out of 256 possible eight-atom supercells) than $L1_2$ (weight of only four configurations), it might represent in some way the solid solution of composition 3:1, especially at elevated temperatures. From this result we can derive a significant increase of the bulk modulus and a small decrease of the lattice parameter when $L1_2$ precipitates are formed. This general trend is confirmed by experiment, as will be discussed in more detail in the Appendix. Of course, this consideration is only a very crude estimate of the properties of a solid solution taking into account only one particular configuration, but the general trend is the same as found from the statistics of supercells[5] and the calculation of the phase diagram.[6] Clearly, a calculation just for the $L1_2$ structure is not sufficient to study the role of the experimentally metastable $L1_2$-Al_3Li compound in realistic alloys.

The calculated bulk modulus of 0.72 Mbar for $L1_2$-Al_3Li agrees well with the experimental value of 0.66 Mbar,[12] especially when one considers the experimental difficulties in measuring a metastable phase formed by precipitation. Most important, according to our re-

TABLE I. Total energy E (Ry) per atom, lattice parameters a (a.u.), atomic radius R (a.u.), bulk modulus B (Mbar), and energy of formation per atom ΔH_f (Ry) for some Al-Li compounds and Al and Li metals and atoms.

Compound		E	a	R	B	ΔH_f
Al_3Li	$L1_2$	−366.5987	7.512	2.935	0.72	−0.0083
Al_3Li	$D0_3$	−366.5887	12.006	2.956	0.52	0.0016
Al_6Li_2	fcc	−366.5954	7.541	2.946	0.62	−0.0051
Al_7Li	fcc	−425.2200	7.519	2.938	0.74	−0.0038
Al_5Li_3	fcc(1)	−307.9707	7.507	2.933	0.52	−0.0063
Al_5Li_3	fcc(2)	−307.9732	7.491	2.927	0.55	−0.0088
Al	fcc	−483.8420	7.538	2.946	0.82	
Li	fcc	−14.8352	8.000	3.126	0.14	
Al	atom	−483.547				
Li	atom	−14.665				

sults[5–7] for all Al-Li compounds, as well as for Al_3Li, the bulk modulus decreases with increasing Li composition, in contrast to the calculation of Ref. 8. This decrease is important for the mechanical properties of Al-Li alloys—as will be considered in Sec. IV. The calculated lattice parameter (7.512 a.u.) is in good agreement with experiment,[13] i.e., 4.01 Å or 7.578 a.u. In this case, our calculated value is smaller by 0.9%; usually, an agreement within 2% is considered to be good. However, one should bear in mind that because of its metastability it is difficult to perform precise measurements of the lattice parameter of δ'-Al_3Li. Furthermore, the consistent underestimation of lattice parameters in many first-principles electronic-structure results might basically arise from neglect of zero-point vibrations.[14] Also, the temperature dependence of the lattice parameter (as well as the bulk modulus) has to be included in comparisons with first-principles calculations that are valid for $T=0$ K.[6] Traditionally, the local-density approximation is held responsible for such deviations from experiment. In view of the points just discussed, however, this does not seem to be well justified—especially when some additional model assumptions (e.g., the atomic-sphere approximation[8]) are made. In choosing the FLAPW method, one is free of such restrictions while paying the higher price for these heavier computations.

B. Bands, density of states, and bonding

In order to analyze the bonding in Al_3Li, we discuss the band structures of compounds with $L1_2$ and $D0_3$ structure in Figs. 3(a) and 3(c). Furthermore, Fig. 3(b) shows bands of pure Al determined with the cubic unit cell of the $L1_2$ lattice containing four Al atoms ("Al_4"). Overall, below the Fermi energy the band structure of $L1_2$-Al_3Li is quite similar to that of Al_4. A distinct difference can be seen for the two lowest bands at the X point [Figs. 3(a) and 3(b)], where a gap opens up in Al_3Li. One might expect this change in the band structure to be due to the Al-Li interactions in the compound, but the Li character of these states is rather weak. For example, only 3% of the second-lowest state at point X is localized in the Li sphere and is mostly due to Al tails dangling into the rather large Li muffin-tin sphere (which is rather large because of its assumed same size as for Al), as described in Sec. II.

Furthermore, by studying the band structure of $Al_3\square$ with a vacancy $\square$, instead of Li we found very much the same features at points X and R in the zone as we did for the $L1_2$-Al_3Li compound. (Because of their similarity, we do not show the band structure of $Al_3\square$.) At the R point in the band structure, four energy levels with degeneracies equal to 3, 1, 1, and 3, which were very close in pure Al, split widely, with the highest level even pushed above E_F. According to our findings, most of these changes come from breaking some of the Al-Al bonds. For pure fcc Al, 12 nearest Al neighbors occur, whereas in the $L1_2$-Al_3Li case, as well as in $L1_2$-$Al_3\square$, only eight Al neighbors remain. A more careful inspection shows that some bands of Al_3Li are lowered in energy. This happens to the bands originating at the second-lowest Γ state as well as at the third-lowest R state, but again, the Li character of the states is rather weak and of the order of a few percent. As for $B32$-LiAl,[7] we argue that Li basically transfers its valence electrons in between the Al atoms. Since we again find for $L1_2$-Al_3Li no particular Li character of the states below E_F, the basic

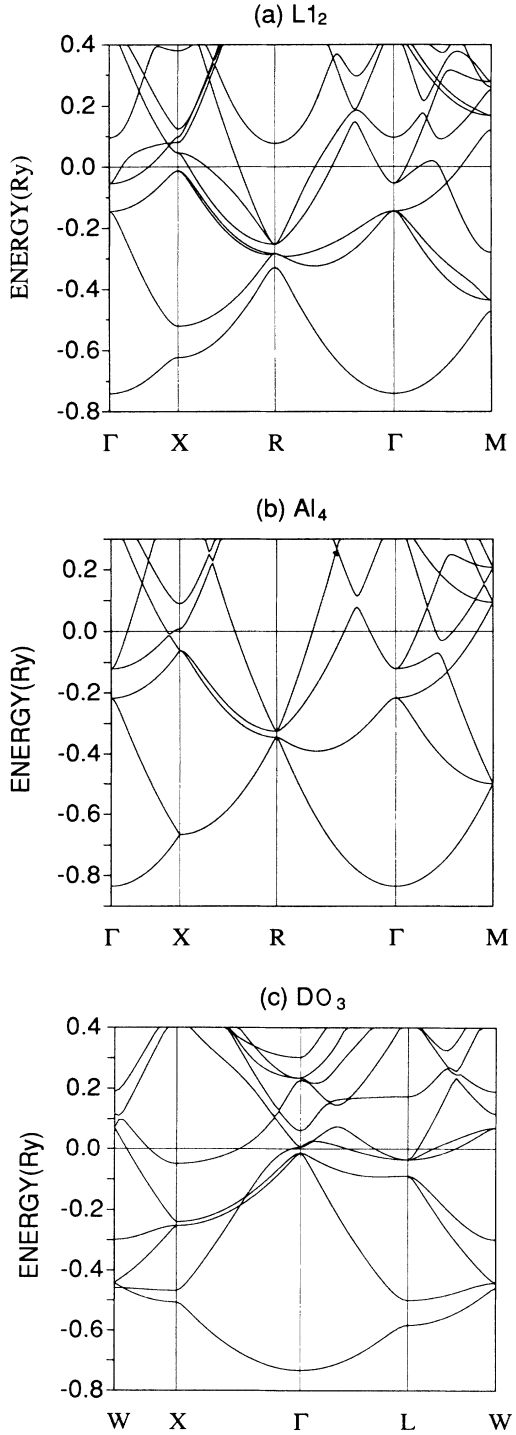

FIG. 3. Band structures of Al_3Li for (a) the $L1_2$ structure, (b) "Al_4" with the four-atom cubic unit-cell treatment of Al metal, and (c) the $D0_3$ structure.

effect of Li seems to be the strengthening of Al bonds. In comparison to $Al_3\square$, the Fermi energy is raised because of the additional Li valence electron which fills more of the states having enhanced Al bonds.

As mentioned above, the fcc-bcc structural competition is a significant feature of the Al-Li phase diagram.[2] The stable structure for LiAl is the bcc-type $B32$ (Zintl) structure (Fig. 1 of Ref. 7), whereas the simplest fcc-type $L1_0$ cannot be stabilized. Focusing on the ordered Al_3Li compounds, the situation reverses because of a very stable $L1_2$ compound relative to the bcc-type $D0_3$ structure which can be constructed by replacing the central Li atom of one of the subcubes of the $B32$ structure by an Al atom (Fig. 1). For this structure there are now two different types of Al atoms, one (type I) with four Al neighbors and tetrahedral bonds as in the $B32$ case, and a second (the center atom, type II) with eight nearest Al neighbors typical for a bcc environment. This mixture of two Al types is clearly shown in the band structure, e.g., by the bands along the $W-X$ direction. Unlike the $B32$ case, which only has flat bands along this direction [Fig. 3(c)], in the $D0_3$ compound these bands arising from the diamond-type tetrahedral bonding of Al type-I atoms are mixed with bands of strong dispersion due to the presence of Al type-II bands of rather free-electron character. Otherwise, the $D0_3$ band structure is very similar to the $B32$ result apart from lifting some degeneracies (e.g., the third-lowest band in the $X-\Gamma$) direction and allowing for some band crossings. The most important point as compared to the LiAl compound is the raising of the Fermi energy.

The density of states (DOS) of the $L1_2$ structure [Fig. 4(a)] below E_F closely resembles that of pure Al, which is essentially a free-electron case modified by some hybridization features. The Li-projected DOS is very small and shows no distinctive features. One interesting point is that E_F falls into a small but distinctive minimum of the DOS, which might indicate the stability of the $L1_2$ structure as compared to the $D0_3$ case [Fig. 4(b)], where E_F cuts through a peak. Figure 4(a) also suggests (assuming a rigid-band model) that the reduction of the number of valence electrons such that E_F falls into the deeper minimum at -0.07 Ry would lead to an even more stable compound. However, removing all the Li from the compound, which leads to the vacancy $Al_3\square$ compound, is too severe because then E_F would already fall into the peak below this minimum. As discussed above, the rigid-band model is a good approximation in our case—as also proven by the fact that the DOS of the $Al_3\square$ compound is practically the same as for Al_3Li below and near E_F.

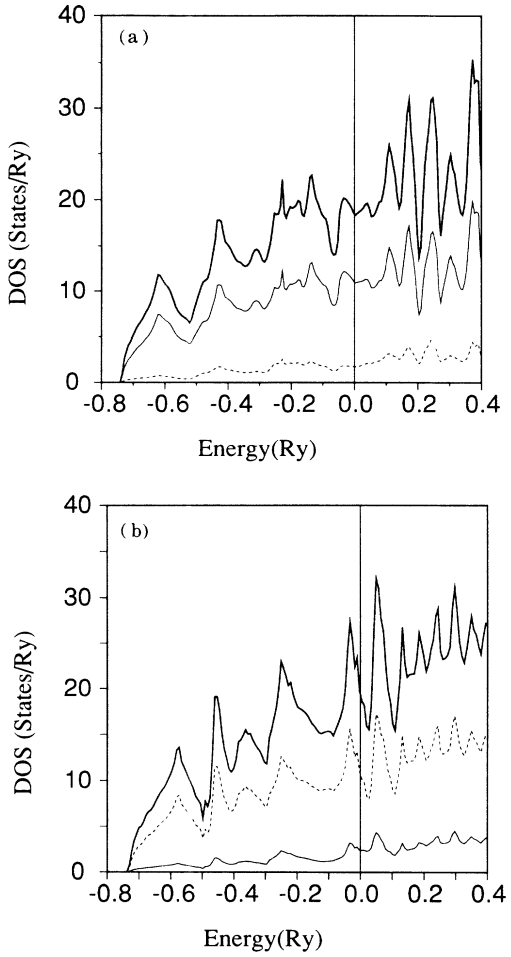

FIG. 4. Density of states $N(E)$ for Al_3Li (in units of states/Ry cell) for (a) the $L1_2$ and (b) $D0_3$ structures. Thick solid line, total $N(E)$; thin solid line, Al; thin dashed line, the Li contributions to $N(E)$.

For the DOS of the $D0_3$ structure [Fig. 4(b)], we find essentially the same features as for the $L1_2$ case, with a

TABLE II. Density of states $N(E_F)$ for the two structures of Al_3Li decomposed into contributions from the interstitial region and from the spheres. The top block (N) corresponds to the density of states at the Fermi energy, and the second block (n) lists the integrated values.

Structure	Total		Al				Li			
	N	N_{int}	N_s	N_p	N_d	N_{sph}	N_s	N_p	N_d	N_{sph}
$L1_2$	17.6	5.3	2.2	6.3	2.0	10.6	0.4	0.9	0.5	1.8
$D0_3$	18.5	5.8	2.9	5.0	2.3	10.3	0.8	1.3	0.3	2.4
	n	n_{int}	n_s	n_p	n_d	n_{sph}	n_s	n_p	n_d	n_{sph}
$L1_2$	10.0	3.0	2.6	2.9	0.4	6.0	0.3	0.5	0.1	0.9
$D0_3$	10.0	3.2	2.7	2.7	0.4	5.9	0.3	0.5	0.1	0.9

minor change in the hybridization features just below E_F. Almost all of the distinctive peaks and minima of the $B32$ LiAl compound [cf. Fig. 5(a) of Ref. 7] are washed out because of the presence of the Al type-II atoms which connect the previously decoupled tetrahedra of the $B32$ structure (if one argues in terms of nearest neighbors only). Table II summarizes some features of the density of states. From the integrated DOS (n) shown by the second (or lower) block, no distinctive difference can be found between the $L1_2$ and $D0_3$ cases. However, from the DOS at E_F, $N(E_F)$ (cf. first or top block), one realizes some important distinctions. $N(E_F)$ is slightly higher for the unstable $D0_3$ case. More interesting is the different orbital character of $N(E_F)$. For the $D0_3$ case we find a distinctive (larger) Li component, reflecting the more isotropic nature of the corresponding states, as also demonstrated by the reduced p character of the Al contribution. It should also be noted that according to Table II, at least at E_F, the Li d character of the states is not negligible, and is larger the more anisotropic the bonding. The Li d character comes from suitable Al states dangling into the Li sphere. It has nothing to do with actual "atomic" d states of Li, which lie high in energy. Thus any calculation which does not take properly into account the $l=2$ components in the Li sphere[8] might lead to bonds that are too isotropic, and therefore it fails to describe the elastic properties in a correct way.

The nature of the bonding is illustrated by the charge density contour plots of Fig. 5. The (100) contour of the $L1_2$ compound [cf. Fig. 5(a)] cuts through a plane of pure Al, as is also found for the LiAl compound of $L1_0$ structure.[7] Because the nearest-neighbor distances are only different by less than 1% (5.278 and 5.312 a.u. for $L1_0$ and $L1_2$, respectively) the contour plots are also very similar and show the pileup of electrons in between the nearest-neighbor Al atoms. For Al_3Li, three such planes (instead of one for $L1_0$) exist, however, in all three main directions, as in pure Al.

Previously (cf. Ref. 7), the stability of the $B32$ structure was attributed to the increased anisotropy of Al bonding, with the Li basically donating its valence electron to strengthen the Al bonds. The bonding in $B32$-AlLi is characterized by strongly directional diamondlike bonds between the Al atoms. Although less pronounced, this general trend is also true for Al_3Li. Figures 5(b) and 5(c) show charge-density-contour plots in the (111) planes for Al_3Li-$L1_2$ and pure Al metal, respectively. In these planes, the charge contours for both the Al-Li and Al-Al nearest neighbors for Al_3Li-$L1_2$ show the formation of more directional Al bonding in Al_3Li-$L1_2$ in comparison with the charge contours for pure Al [Fig. 5(c)]. In pure Al, as expected, the charge is more homogeneously distributed spatially. In Al_3Li-$L1_2$, however, we see more of a pileup of charge in the Al bonds, whereas the charge density between Al and Li atoms decreases monotonically (from Al to Li). Further, the increased anisotropy with the addition of Li can be seen from the ratio of higher-l components to the $l=0$ component of the charge density in the muffin tins for pure Al (0.053) and the compound (0.144). The unusual elastic properties in Al-Li alloys (i.e., the increase of Young's modulus with the decrease

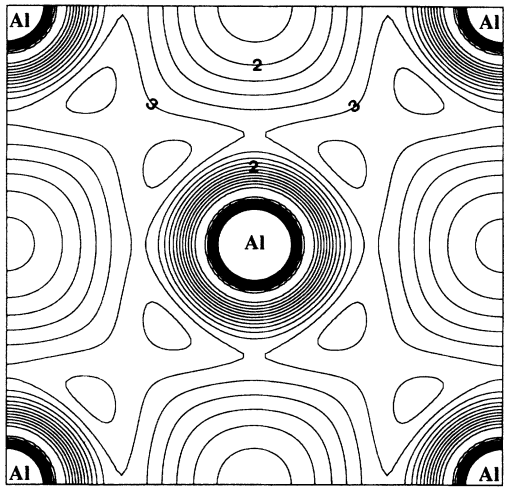

(a) $L1_2$ (100)

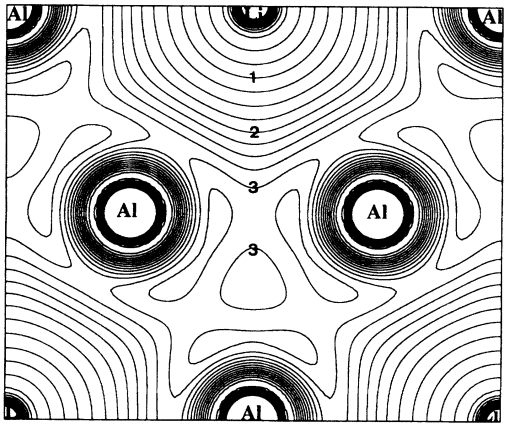

(b) $L1_2$ (111)

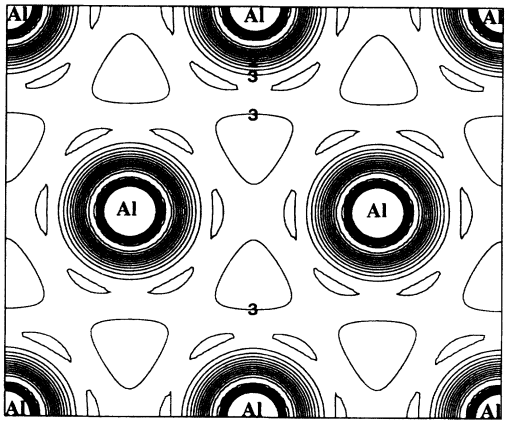

(c) Al (111)

FIG. 5. Charge-density-contour plots for the $L1_2$ structure [(a) and (b)], and pure Al [(c)] in units of 10^{-2} [(number of electrons)/(a.u.)^3].

of bulk modulus) can therefore be attributed to the increased anisotropic bonding in the Al-Li alloys, as will be discussed later. The much more pronounced directional bonding between Al atoms was also found for two stable Li-rich Al-Li compounds, i.e., Al_2Li_3 and Al_4Li_9.[15]

IV. Al_3Li AND THE Al-Li PHASE DIAGRAM

Al_3Li is found to be metastable with respect to an Al-rich solid solution and the LiAl ordered compound of $B32$ structure.[2] From our results for the ordered compounds fcc-Al, $L1_2$-Al_3Li, and $B32$-LiAl, we can derive the metastability. Considering the energy of formation per atom, $\Delta H_f(x)$, as a function of Li composition x, we find that the value for Al_3Li (-8.4 mRy) lies exactly on the line connecting $[\Delta H_f(0)=0]$ (pure Al) with $[\Delta H_f(0.5)=-16.8$ mRy] (LiAl). (Note that Table I of Ref. 7 lists energies per LiAl pair and thus these energies have to be divided by 2.) At $T=0$ K the three phases are therefore equally stable. Lying on a common tangent of the free energy with increasing temperature and entropy of mixing, the free energy of the solid solution at the very-Al-rich side is lowered more than the free energy of the ordered Al_3Li and $B32$ phases. As a result, the free energy of Al_3Li is above the common tangent, and it is no longer stable; however, it might become metastable if it stays close enough to the common tangent. This actually happens when a proper model of the solid solution is taken into account.[6] Experimentally, up to 50% of the alloy volume can be transformed into Al_3Li precipitates by solution annealing and artificial aging.[3] Such an amount of coherent precipitations is unusually high and has not been obtained for any other Al alloy so far.

Our first-principles calculations provide the information that no other stable phase exists in the Al-rich side of the phase diagram. Applying the results of Table II, one finds that at $T=0$ K the fcc supercell compound Al_7Li situated between pure Al and Al_3Li lies slightly above (by 0.4 mRy) the common tangent connecting Al and Al_3Li. On the other side, the energy of formation of the Al_5Li_3 supercell compounds (two different fcc configurations of nearly equal statistical weights exist for the 5:3 composition) lies well above the common tangent of Al_3Li and LiAl, indicating the high stability of $B32$-LiAl. If one only studies fcc metastable phase stabilities[5] by neglecting the bcc-type $B32$ results, we find that Al_5Li_3 is also not stable as compared to Al_3Li and LiAl (with fcc $L1_0$ structure); this reflects the tendency of Al-rich Al-Li alloys to form ordered compounds with small unit cells.

A further important quantity for the formation of the Al_3Li compound is the lattice mismatch as defined by $\delta=(a_{Al_3Li}/a_{SS}-1)\times 100\%$. The mismatch between solid solution, a_{SS}, and precipitate, a_{Al_3Li}, must be sufficiently small. Comparing Al_3Li to pure Al, Al_7Li, and Al_6Li_2, the mismatch varies in the range $-0.38\le\delta\le-0.09$. Of course, for a precise definition a model of the solid solution had to be developed[5,6] that gives essentially similar results. The experimental values[16] show some scattering but, in principle, support our results, namely a small but negative mismatch.

The elastic properties of the Al-Li alloys are of special interest because, in general, Li additions increase Young's modulus (or related quantities such as stiffness) up to 25% (compared to 0.66 Mbar for pure Al) for Li compositions of about 10%.[17,18] The contribution of Al_3Li precipitates to this increase of Young's modulus in technological alloys was estimated to be about 20%;[17] the rest was ascribed to the hardening of the Al-Li solid solution. However, for Al_3Li an experimental modulus of 0.96 Mbar (Ref. 17) is given, which corresponds to an increase of 45%. Therefore, procedures which produce the largest amount of Al_3Li precipitates (e.g., by high cooling rates) "make the most of the potential of Li additions to increase the specific strength and Young's modulus, in contrast to the melt-metallurgical route."[3] On the other hand, according to the generally accepted experimental results of Müller *et al.*,[12] the bulk modulus decreases with increasing Li composition. Our calculated results show a general decrease of the bulk modulus with increasing Li composition for all Al-Li compounds. The increase of the Young's modulus therefore has to be ascribed to the increasing anisotropy of the electronic bonding in the material, which is beautifully illustrated by the diamondlike bonds (concerning the geometry but, of course, not the strength) in $B32$-LiAl.[7]

Interestingly, although the bulk modulus of LiAl is substantially decreased, as found by two calculations [0.58 (Ref. 7) and 0.45 Mbar (Ref. 17)], its Young's modulus was measured to be 1.05 Mbar,[17] as compared to pure Al (0.66 Mbar) and Al_3Li (0.96 Mbar). These results indicate that the Poisson ratio has to decrease rapidly—as found experimentally, although some ambiguities remain.[19] Estimating the Poisson ratio from our calculated bulk moduli B and the measured Young's moduli E, we find a ratio of 0.366 for pure Al ($B=0.82$ Mbar, $E=0.66$ Mbar), which decreases to a value of 0.275 for Al_3Li ($B=0.72$ Mbar, $E=0.96$ Mbar). By linear extrapolation of these values to LiAl, one obtains a Poisson ratio of 0.184, which is very close to the ratio derived in the same way as before ($B=0.58$ Mbar, $E=1.05$ Mbar). These results support, at least partially, the experimental findings of Glazer and Morris.[19] From Table I one finds that, in general, all our results show a decreasing bulk modulus with increasing Li composition, although it might vary considerably for the 3:1 composition—which emphasizes the special role of Al_3Li in strengthening the alloy. Note that the bulk modulus of the $D0_3$ structure does not fit into this scheme because of the unfavorable bonding in this compound. The outstanding role of the very stable LiAl $B32$ compound can be deduced from its bulk modulus (0.58 Mbar), which is higher than the moduli of the 5:3 compounds (0.52 and 0.55 Mbar, respectively).

Finally, we have completed some first-principles FLAPW calculations for the elastic constants of Al_3Li. From these we obtain a Young's modulus of 1.20 Mbar, which matches reasonably well the experimental value of 0.96 Mbar,[17] taking into account the experimental uncertainties and temperature effects. The calculated Young's modulus is about 60% larger than the bulk modulus of

0.72 Mbar (Sec. III A), as derived from the same first-principles method. Clearly, our results support the well-established view that adding Li to Al (at the Al-rich side) strengthens the alloy by strongly increasing its anisotropic mechanical properties, although the isotropic bulk modulus is reduced.

V. CONCLUSIONS

We have studied the cohesive, electronic bonding properties and structural stability of the binary compound Al_3Li. The fcc-based $L1_2$ structure is found to be stable relative to the bcc-based $D0_3$ structure. In the Al-Li phase diagram the metastability of the $L1_2$ phase can be described by its calculated heat of formation with respect to that of the most stable $B32$-LiAl phase. The bulk modulus is found to be generally decreased with the increase of Li content, and the increase in Young's modulus reveals the anisotropic properties of Al bonding in the Al-Li systems, e.g., the decrease of Poisson's ratio. The energetic and equilibrium properties appear to be in good agreement with experiment.

ACKNOWLEDGMENTS

This work was supported by the Air Force Office of Scientific Research (Grant No. 88-0346), U.S. Department of Defense, a computing grant at the Wright-Patterson Air Force Base Supercomputing Center, and the Austrian Ministry of Science (Project No. 49-55313-24187).

APPENDIX: COMPARISON WITH ASW AND LMTO RESULTS

The important point derived from studying the electronic structure of Al-Li alloys seems to be the anisotropic bonding between the Al atoms, whereas Li basically donates its valence electron to strengthen the Al bonds, as already discussed for LiAl.[7,20] From such a point of view, one would understand the anisotropic behavior as expressed by the decrease of the bulk modulus with increasing Li composition (as found by our calculations and by experiment[12], but an increase of Young's modulus, as found by all experiments (e.g., Ref. 16). Recently, some first-principles calculations for Al_7Li and Al_3Li (as well as for other Al compounds) were published,[8] which claim that the bulk modulus increases with Li composition, and therefore the increase of Young's modulus could be understood by applying the theory of isotropic elastic media. These authors claimed that our results (our eight-atom supercell study had been published[5]) are not consistent with their findings, but did not discuss its possible cause.

To clarify this point, we focus here in detail on Al_3Li with the $L1_2$ structure, which can be easily used as a test case because of its simple structure—having four atoms in a cubic unit cell [cf. Fig. 1(a)]. In order to test our FLAPW calculation further, we increased the basis set by a factor of 2 from 50 augmented plane waves per atom (200 in total) to 100 (400 in total). As we knew from previous tests and studies,[7] the smaller set is sufficiently large because of the delocalized plane-wave-like nature of the basis functions. As expected, the total energy changed by a very small amount (about -0.1 mRy) in a uniform way. Therefore, both the lattice parameter and bulk modulus remain unchanged. As mentioned in Sec. II, the total energy as a function of the number of **k** points was also converged; 60 **k** points were found to be sufficient for obtaining precise bulk-modulus and lattice-parameter values. Further, using the FLAPW method we find (Table I) at equilibrium an energy of formation of -8.4 mRy, a lattice parameter of 7.512 a.u., and a bulk modulus of 0.72 Mbar. Masuda-Jindo and Terakura[8] find -9 mRy, 7.424 a.u., and 0.96 Mbar, respectively. [These data were taken directly or derived from their Table I using their Eqs. (2) and (3).] The most striking difference can be found for the bulk modulus, but the lattice parameters are also different, with ours being more than 1% larger. For Al_7Li (cf. Table I) the situation is similar apart from the energy of formation, for which Masuda-Jindo and Terakura list a value that must be too large by a factor of 2 because, according to their Table I, it should be -8.5 mRy per atom [the value listed is -0.034 for $(Al_7Li)/2$]. If that is the case, then Al_3Li would never be formed for Li compositions smaller than 12.5%.

At first, the basic difference between the two calculations is the model applied. In our case we applied the FLAPW method, which is one of the most precise methods available because it is an all-electron method that does not make any shape approximations for the potential and charge density. On the other hand, Masuda-Jindo and Terakura applied the ASW method[21] (which basically is very similar to the LMTO method,[10] which uses the muffin-tin approximation for the charge density and potential). (Every atom in the cell is surrounded by a muffin-tin sphere in such a way that the sum of the sphere volumes equals the volume of the unit cell. Of course, this results in overlapping spheres, and also a choice for the radius of the spheres has to be made if there is more than one atom per unit cell, and especially if there are different species of atoms as in our case.) Now it is well known that for close-packed structures the ASW and LMTO methods give, in general, good results (with very few exceptions) as compared to experiment and other results of precise methods. Therefore the discrepancy between the FLAPW and ASW results of Ref. 8 is hard to understand at first.

To further investigate this difference between the FLAPW and ASW results, we carried out some LMTO calculations using the atomic radii for each element as a function of lattice parameter (volume) obtained by Masudo-Jindo and Terakura[8] using the bulk modulus of each elemental metal. (The unpublished values were kindly provided by Professor Terakura.) These calculations were done self-consistently in the usual way for their set of four different lattice parameters, and 60 (and up to 205) **k** points were used for the Brillouin-zone integration by the linear tetrahedron method. Both the bulk modulus and equilibrium lattice parameter did not change by taking more than 60 **k** points. Two sets of calculations were performed with $l_{max}=1$ (as done in Ref. 8) and $l_{max}=2$ for Li, and with the combined-correction

terms (included in the ASW calculations).[22] Calculations carried out without combined-correction terms did not yield an equilibrium distance (i.e., minimum in the total energy) for the sphere radii used in Ref. 8. The reason that l_{max} for Li was increased over the value used in Ref. 8 is that the choice of Li-sphere radius is rather large for a Li, ion and the tails of the Al wave functions reach deep inside the Li sphere. As we learned from the FLAPW results (see Sec. III B and Table I), the bonding is rather anisotropic and hence $l=2$ components inside the Li sphere may be important. Results at the equilibrium lattice constant given in Table III (as Calc. 1 and Calc. 2) show strong differences for the calculated total energies and lattice constants. The bulk-modulus values are reasonably close to each other—and close to our earlier FLAPW result. Thus, we do not reproduce the high value of the bulk modulus (~ 1.0 Mbar) obtained previously.[8]

Summarizing, based on our rather detailed studies we believe that our FLAPW results are reliable, correct, and consistent. In Ref. 8 some experimental studies were used to corroborate the ASW results. However, without going into detail here, there are at least as many reliable experimental statements (we refer to Sec. IV and the discussion in Ref. 6 that support our basic finding, namely that the Al-Li alloys and compounds are rather anisotropic and reveal a decreasing bulk modulus with increasing Young's modulus. In consequence, their elastic properties could only be described by a strongly decreasing Poisson ratio. This conclusion is confirmed by the calculated Young's modulus, which is about 60% larger than the bulk modulus.

TABLE III. Results of LMTO calculations for $L1_2$-Al_3Li using the sphere radii of Ref. 8. Calc. 1 includes $l_{max}=2$ and Calc. 2 includes $l_{max}=1$ for Li. In both cases, $l_{max}=2$ for Al. Total energy E (in Ry/atom), lattice constant a (in a.u.), and bulk modulus B (in Mbar).

	E	a	B
Calc. 1	−366.579	7.452	0.68
Calc. 2	−366.586	7.547	0.76

*Present address: Institute of Physics Chemistry, University of Vienna, Währingerstrasse 42, A-1090 Vienna, Austria.

[1]T. H. Sanders, Jr. and E. A. Starke, Jr., *Aluminum-Lithium Alloys* (The Metallurgical Society of AIME, New York, 1981); T. H. Sanders, Jr. and E. A. Starke, Jr., *Aluminum-Lithium Alloys II* (The Metallurgical Society of AIME, New York, 1984); C. Baker, P. J. Gregson, S. J. Harris, and C. J. Peel, *Aluminum-Lithium Alloys III* (The Institute of Metals, London, 1986).

[2]F. W. Gayle and J. B. van der Sande, Bull. Alloy Phase Diagrams **5**, 19 (1984).

[3]W. Schlump and H. Grewe, Aluminum **63**, 1024 (1987).

[4]E. J. Lavernia and N. J. Grant, J. Mater. Sci. **22**, 1521 (1987).

[5]R. Podloucky, H. J. F. Jensen, X.-Q. Guo, and A. J. Freeman, Phys. Rev. B **37**, 5478 (1988).

[6]M. Sluiter, D. de Fontaine, X.-Q. Guo, R. Podloucky, and A. J. Freeman (unpublished).

[7]X.-Q. Guo, R. Podloucky, and A. J. Freeman, Phys. Rev. B **40**, 2793 (1989).

[8]K. I. Masuda-Jindo and K. Terakura, Phys. Rev. B **39**, 7509 (1989).

[9]H. J. F. Jansen and A. J. Freeman, Phys. Rev. B **30**, 561 (1984).

[10]O. K. Andersen, Phys. Rev. B **12**, 3060 (1975).

[11]L. Hedin and S. Lundqvist, J. Phys. C **4**, 2064 (1971).

[12]W. Müller, E. Bubeck, and V. Geroald, in *Aluminum-Lithium Alloys III*, edited by C. Baker, P. J. Gregson, S. J. Harris, and C. J. Peel (Institute of Metals, London, 1986), p. 435.

[13]S. Kang and N. J. Grant, in *Aluminum-Lithium II*, edited by E. A. Starke, Jr. and T. H. Sanders, Jr., (The Metallurgical Society of AIME, New York, 1983), p. 469.

[14]V. L. Moruzzi, J. F. Janak, and K. Schwarz, Phys. Rev. B **37**, 790 (1988).

[15]X.-Q. Guo, R. Podloucky, and A. J. Freeman (unpublished).

[16]M. Tamura, T. Mori, and T. Nakamura, J. Jpn. Inst. Metals **34**, 919 (1970); B. Noble and G. E. Thompson, Metals Sci. J. **5**, 114 (1971); D. B. William and J. W. Edgington, Metals Sci. J. **9**, 529 (1975); S. F. Baumann and D. B. Williams, in *Proceedings of the 2nd International Conference on Aluminum-Lithium Alloys*, edited by T. H. Sanders, Jr. and E. A. Starke, Jr. (The Metallurgical Society of AIME, Warrendale, PA, 1986), Vol. 17.

[17]B. Noble, S. J. Harris, and K. Dinsdale, J. Mater. Sci. **17**, 461 (1982).

[18]F. H. Samuel and G. Champier, J. Mater. Sci. **22**, 3851 (1987).

[19]J. Glazer and J. W. Morris, Am. Inst. Aeron. Astronautics J. **25**, 1271 (1987).

[20]N. E. Christensen, Phys. Rev. B **32**, 207 (1985).

[21]A. R. Williams, J. Kübler, and C. D. Gelatt, Jr., Phys. Rev. B **19**, 6094 (1979).

[22]Calculations without the combined-correction terms yielded unphysical results—as expected from the work of Williams, Kübler, and Gelatt, Jr. (Ref. 21).